The nuclear symmetry energy and the breaking of isospin symmetry

Can we reconcile our understanding of the symmetry energy with the isobaric analog state properties? => Isospin breaking nuclear forces

November 20th, 2018, RIKEN, Japan

H. Sagawa RIKEN/University of Aizu

In collaborations with Xavier Roca-Maza and Gianluca Colo, Milano

PHYSICAL REVIEW LETTERS **120,** 202501 (2018)

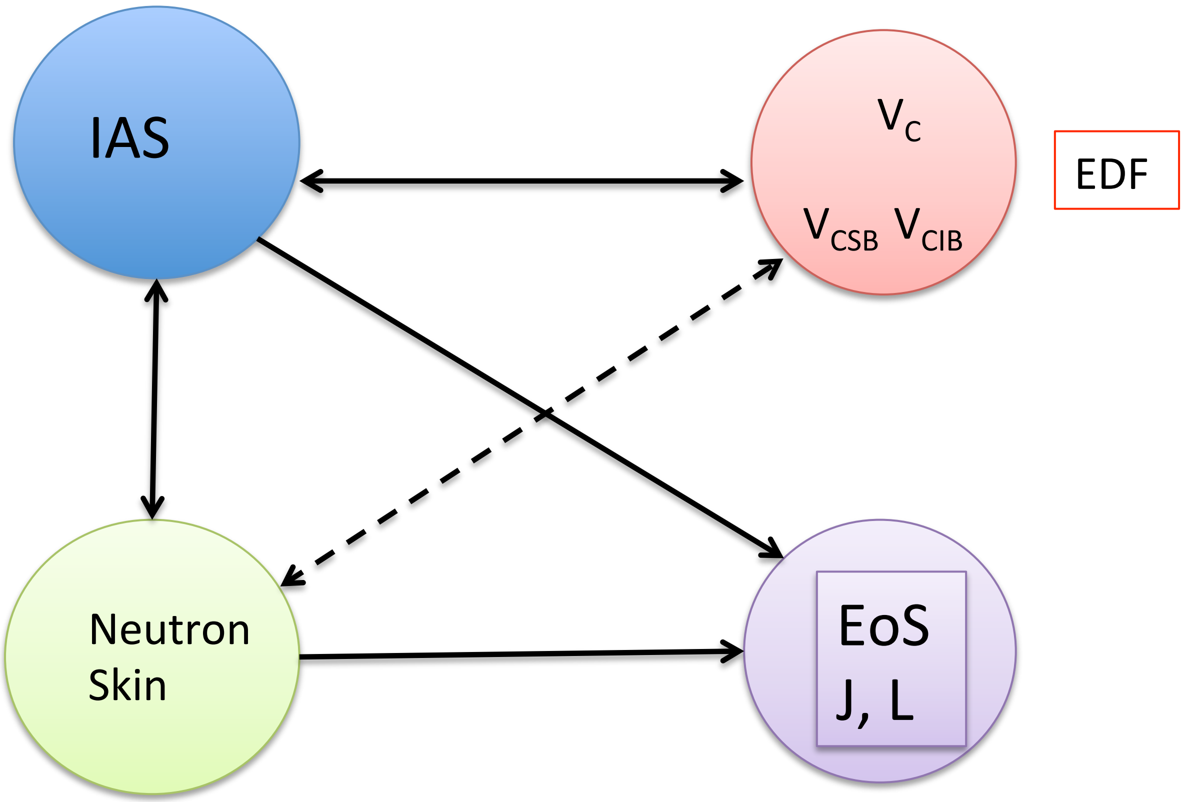

IAS
V_C
V_{CSB} V_{CIB}
EDF
Neutron Skin
EoS
J, L

The Nuclear Equation of State: Infinite System

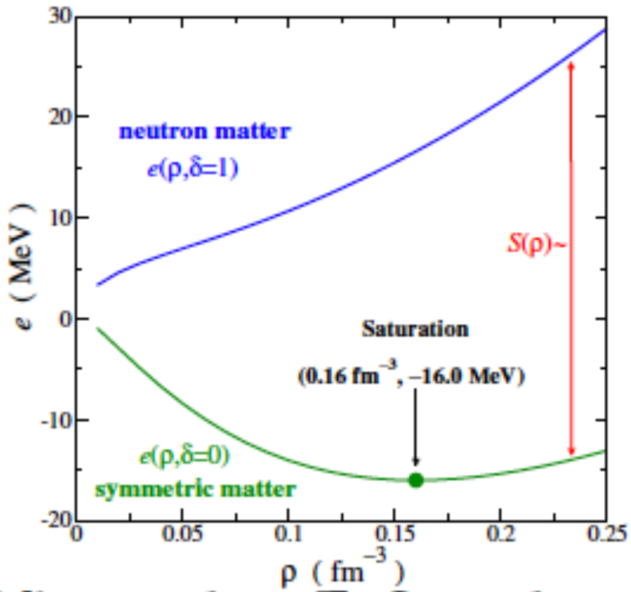

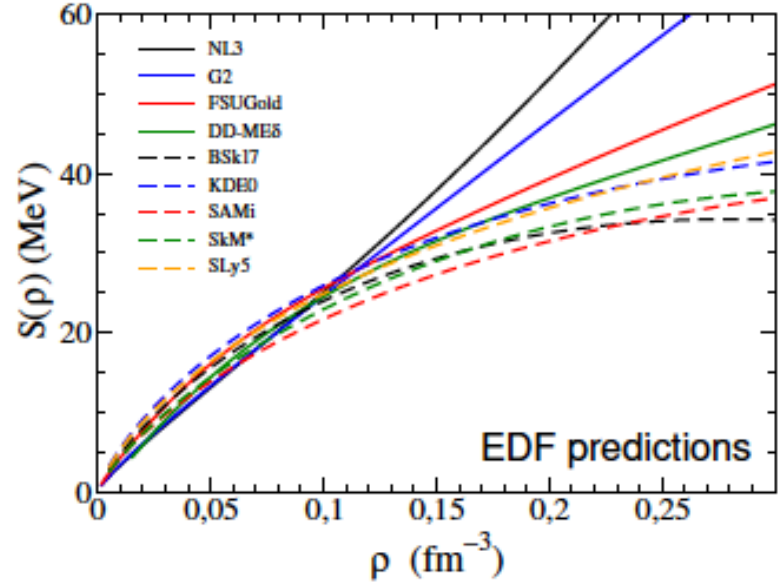

* The nuclear EoS can be written in good approximation as:

E/A= $e(\rho,\beta) \approx e(\rho,\beta=0) + S(\rho)\beta^2$ where $\beta \equiv \dfrac{\rho_n - \rho_p}{\rho_n + \rho_p}$

* SNM can be expanded around ρ_0 and define some useful parameters:

$$S(\rho) = J + L\left(\frac{\rho-\rho_0}{3\rho_0}\right) + \frac{1}{2}K_{sym}\left(\frac{\rho-\rho_0}{3\rho_0}\right)^2$$

where $J = S(\rho_0)$, $L = 3\rho_0 \left.\dfrac{\partial S}{\partial \rho}\right|_{\rho_0}$, $K_{sym} = 9\rho_0^2 \left.\dfrac{\partial^2 S}{\partial \rho^2}\right|_{\rho_0}$

Examples: EoS parameters from nuclear observables

Isovector properties (e.g. $S(\rho)$) are thought to be well determined by the **neutron skin thickness** ($\Delta r_{np} \equiv \langle r_n^2 \rangle^{1/2} - \langle r_p^2 \rangle^{1/2}$) **of a heavy nucleus such as ^{208}Pb)**:

Macroscopic model: $\Delta r_{np} \sim \frac{1}{12} \frac{(N-Z)}{A} \frac{R}{J} L \quad (L \propto p_0^{neut})$

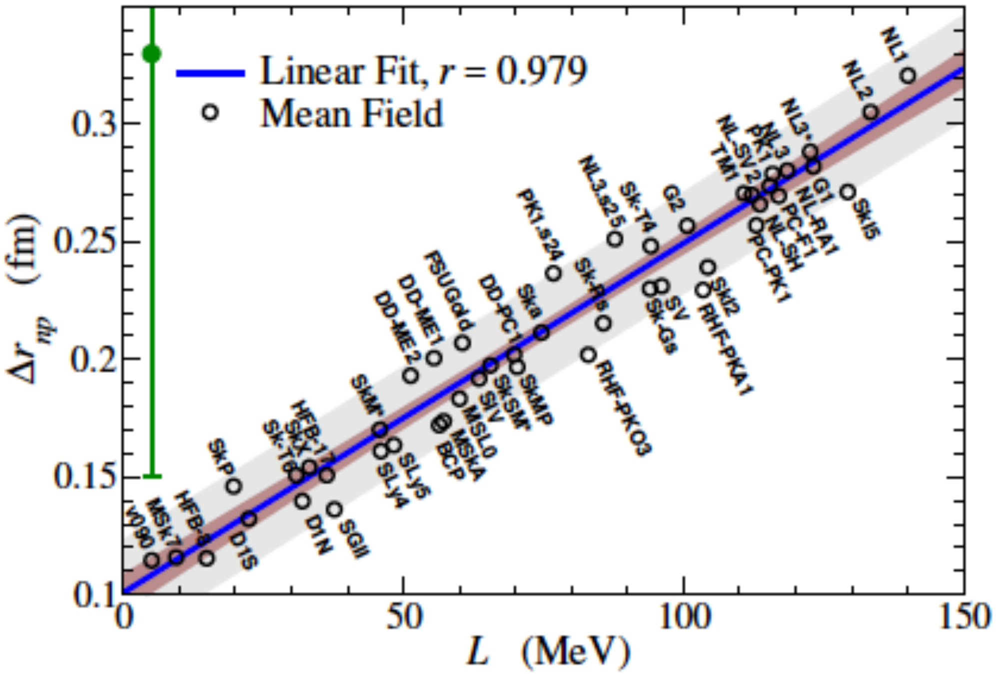

Micorscopic models (EDFs) confirm such a relation

However the experimental precision and accuracy needed in the measurment of this property is very challenging nowadays.

Physical Review Letters **106**, 252501 (2011)

[Exp. from strongly interacting probes: $\sim 0.15 - 0.22$ fm (*Physical Review C* **86** 015803 (2012))].

Isospin proposed by W. Heisenberg (1932)

Isospin conservation $[H,T]=0$

$$[H,T]=[V_C,T]\neq 0$$

But the violation is rather small.

$$[H,T]=[V_C+V_{CSB}+V_{CIB},T]\neq 0$$

Existence of Isobaric Analog States
(Experimental Evidence by charge exchange reaction)

J.D. Anderson, C. Wong and J.W. McClure: Phys. Rev. Letters **7** (1961) 250; Phys. Rev. **126** (1962) 2170; Phys. Rev. **129** (1963) 2718.

Bohr-Mottelson: Isospin violation

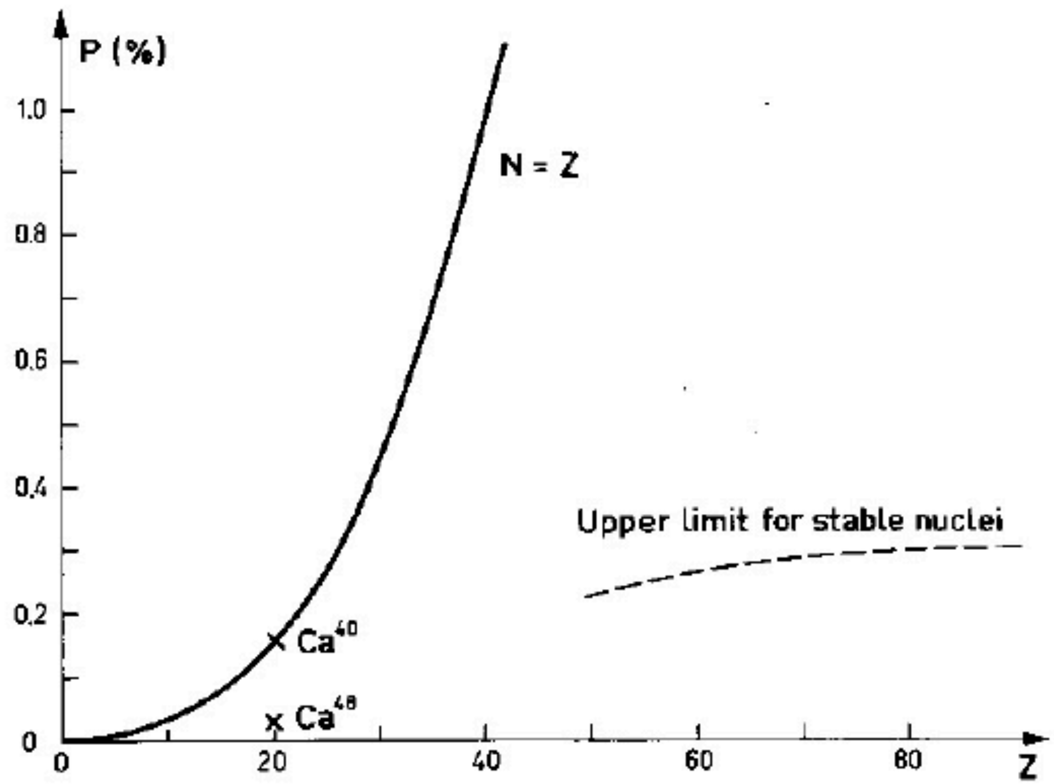

Figure 2-6 The figure shows the isospin impurities in nuclear ground states estimated on the basis of the hydrodynamical model (A. Bohr, J. Damgaard, and B. R. Mottelson, in *Nuclear Structure*, p. 1, eds. A. Hossain, Harun-ar-Rashid, and M. Islam, North-Holland, Amsterdam, 1967.)

▼ and $T_0 + 1$, and we obtain

$$P(T_0+1) = \langle T_0 T_0 1 0 | T_0+1, T_0\rangle^2 P(\tau=1) = (T_0+1)^{-1} P(\tau=1) \quad (2\text{-}108)$$

The isobaric analog state energy: ΔE_d

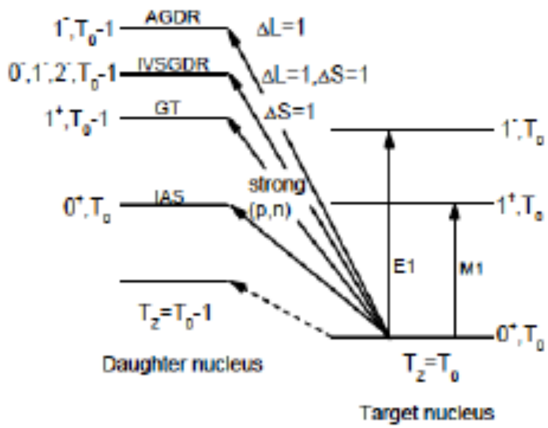

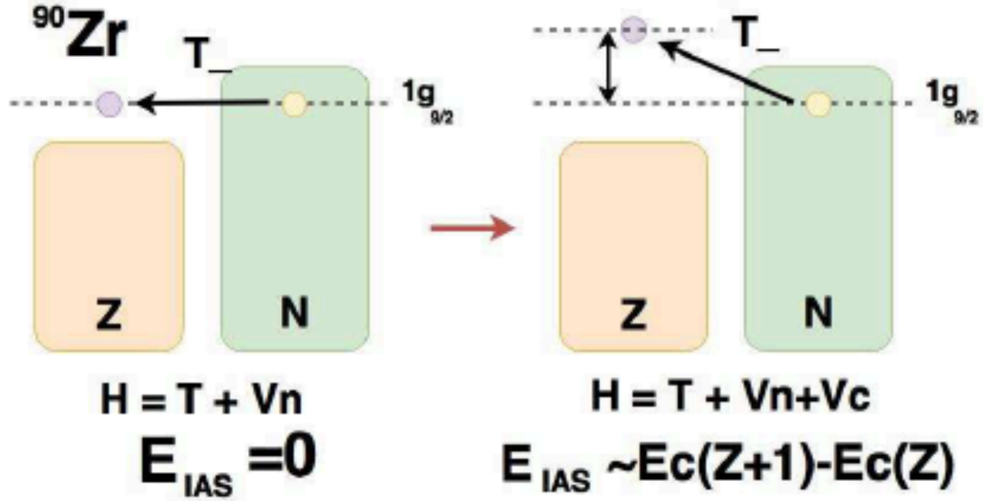

- **Definition:** $(N, Z+1) \to (N+1, Z)$: T_0 g.s. isospin of $(N+1, Z)$, its IAS in $(N, Z+1)$ will be the lowest state where $T = T_0$.
- **Analog state** can be defined: $|A\rangle = \dfrac{T_-|0\rangle}{\langle 0|T_+T_-|0\rangle}$
- **Displacement energy**

$$E_{IAS} \approx \Delta E_d \equiv E_A - E_0 = \langle A|\mathcal{H}|A\rangle - \langle 0|\mathcal{H}|0\rangle = \frac{\langle 0|[T_+[\mathcal{H}, T_-]]|0\rangle}{\langle 0|T_+T_-|0\rangle}$$

E_{IAS}^{exp} easy to measure and depends only on isospin symmetry symmetry breaking terms: Coulomb and to less extent (few %) strong interaction

Nuclear Physics A526 (1991) 1–35

Indiana Cyclotron

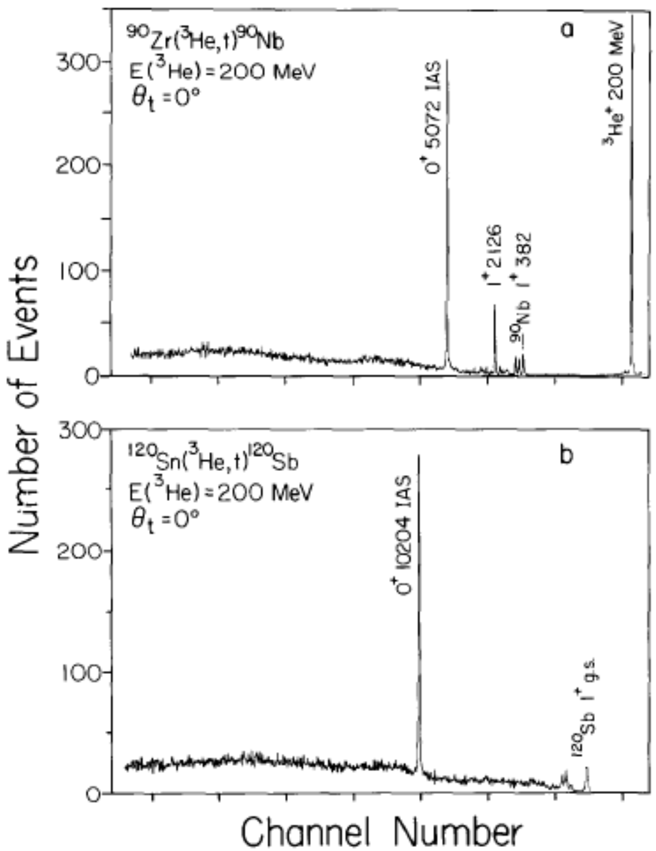

Fig. 7. Triton energy spectra from the (^{3}He, t) reaction of $E(^3\text{He}) = 200$ MeV and $\theta_t = 0°$ for targets (a) ^{90}Zr, (b) ^{120}Sn. Excitation energies are given in keV.

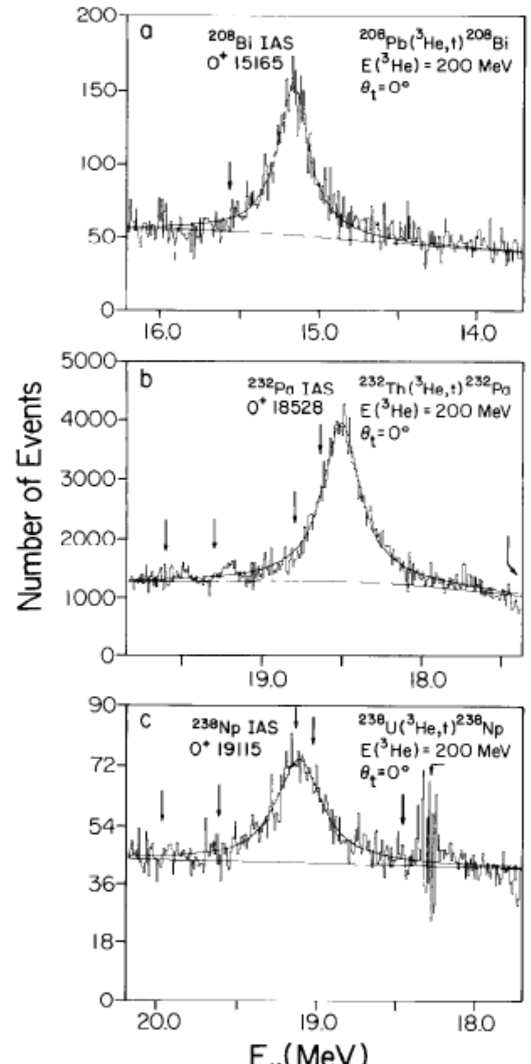

Fig. 10. Triton energy spectra (expanded scales) corrected for background obtained for the IAS in (a) ^{208}Bi, (b) ^{232}Pa and (c) ^{238}Np at $E(^3\text{He}) = 200$ MeV, $\theta_t = 0°$ with lorentzian line shape fitting. Irregular patterns appear where contributions from ^{12}C and ^{16}O contaminants are subtracted. The locations are marked by arrows.

Coulomb direct displacement energy

$$\left\langle \left[T_+ , [H, T_-] \right] \right\rangle \Rightarrow$$

$$\Delta E_d \approx \Delta E_d^{C,\text{direct}} = \frac{1}{N-Z} \int [\rho_n(\vec{r}) - \rho_p(\vec{r})]\, U_C^{\text{direct}}(\vec{r}) d\vec{r}$$

where $U_C^{\text{direct}}(\vec{r}) = \int \frac{e^2}{|\vec{r}_1 - \vec{r}|} \rho_{ch}(\vec{r}_1) d\vec{r}_1$

Assuming a uniform neutron and proton distributions of radius R_n and R_p respectively, and $\rho_{ch} \approx \rho_p$ one can find

$$\Delta E_d \approx \Delta E_d^{C,\text{direct}} \approx \frac{6}{5} \frac{Ze^2}{R_p} \left(1 - \frac{1}{2} \frac{N}{N-Z} \frac{R_n - R_p}{R_p} \right)$$

One may expect: **the larger the Δr_{np} the smallest E_{IAS}**

COULOMB ENERGIES AND THE EXCESS NEUTRON DISTRIBUTION FROM THE STUDY OF ISOBARIC ANALOG RESONANCES†

Naftali Auerbach, Jörg Hüfner, A. K. Kerman, and C. M. Shakin

	$\|\pi>$ Parent State	Ca^{49}	Sr^{89}	Ba^{139}	Pb^{209}
E_R-E_A	Contin.-Comp. Mixing	-0.06	-0.10	-0.17	-0.48
	Dyn. p-n Mass Effect	0.04	0.04	0.04	0.04
	El.Magn. Spin Orbit	-0.07	-0.08	-0.01	-0.02
$\Delta E_d^{C.D.}$	Estimate Eq. (5)	-0.20	-0.16	-0.23	-0.25
	Phenomen. Force	-0.02	-0.16	—	—
ΔE_d^{Coul}	Direct Term	7.60	12.10	15.46	19.95
	Exchange Term	-0.31	-0.35	-0.35	-0.35
$\Delta E_d^{F.S.}$	Finite Proton Size	-0.10	-0.11	-0.11	-0.11
ΔE_d^{CORR}	Short Range Correlat.	~0.1	~0.1	~0.1	~0.1
ΔE_d^{T-IMP}	Collective Model	-0.01	-0.04	-0.06	-0.09
E_R-E_π	Theory	7.08±.20	11.40±.25	14.67±.25	18.79±.25
	Experiment	7.083±.015 (a)	11.40±.02 (a)	14.67±.02 (a)	18.790±.013 (b)
c_o [fm]	Charge Distribution	1.03	1.08	1.09	1.12
t [fm]	Charge Distribution	2.3	2.3	2.3	2.2
r_o [fm]	Neutron Potential	1.06±.08	1.10±.05	1.11±.05	1.12±.04
R_{rms} [fm]	Excess Neutrons	3.71±.18	4.36±.15	4.99±.15	5.63±.15
	Protons	3.42	4.10	4.75	5.42
	All Neutrons	3.51±.04	4.17±.05	4.83±.05	5.50±.05

E_{IAS} in Energy Density Functionals (No Corr.)

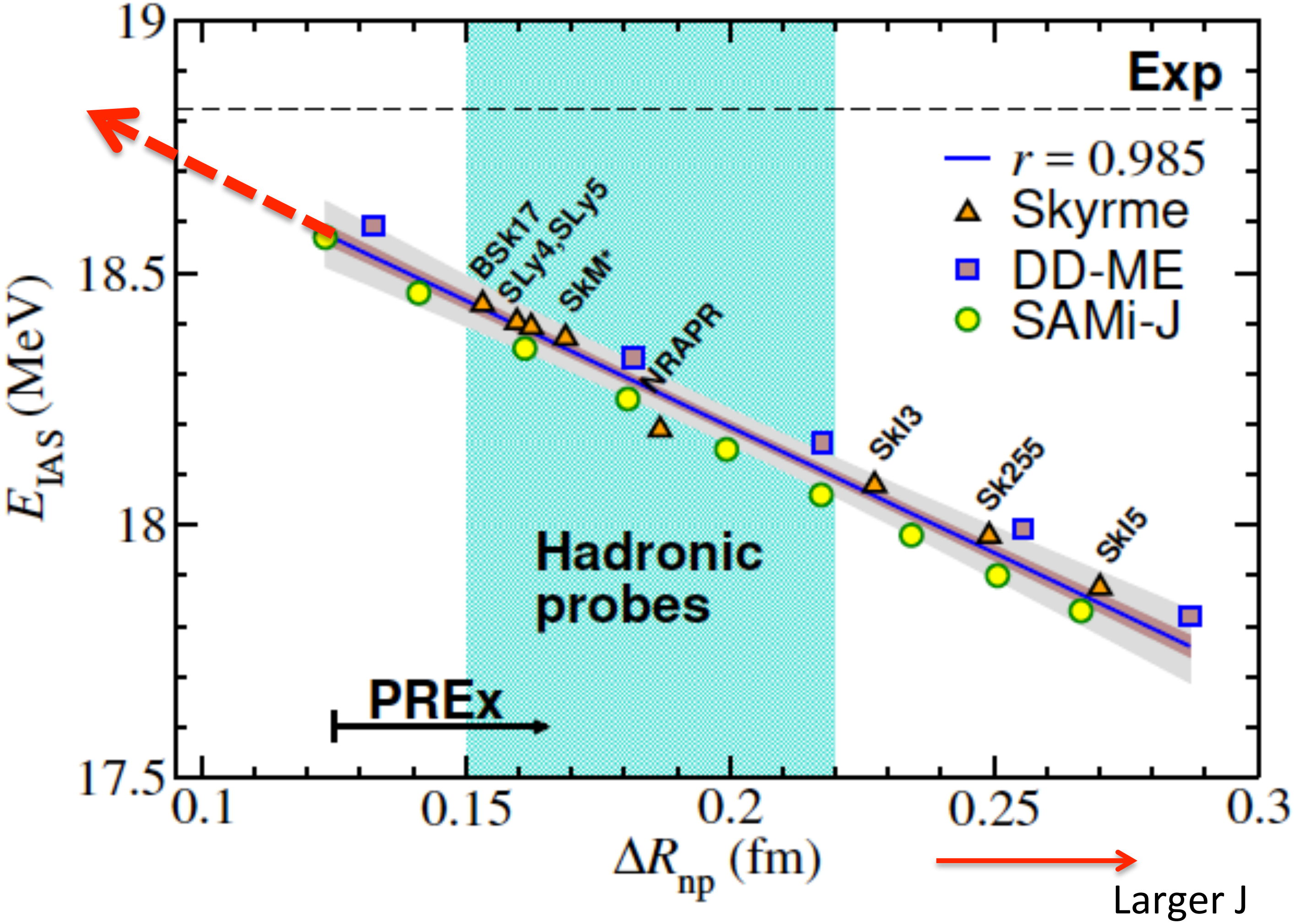

EDFs derived from Hartree-(Fock) + Random Phase approximations using relativistic (and non-relativistic) interactions where the nuclear part is isospin symmetric and U_{ch} is calculated from the ρ_p

How can we reconcile this contradiction between IAS energy and neutron skin?

For the first time within self-consistent

HF+RPA

" a state of the art" calculation"

Within the **HF+RPA** one can **estimate** the E_{IAS} accounting (in an effective way) for **short-range correlations, isospin impurities and effects of the continuum** (if a large sp base is adopted).

- **Coulomb exchange** exact (usually Slater approx.):

$$U_C^{x,exact}\varphi_i(\vec{r}) = -\frac{e^2}{2}\int d^3r' \frac{\varphi_j^*(\vec{r}')\varphi_j(\vec{r})}{|\vec{r}-\vec{r}'|}\varphi_i(\vec{r}')$$

- The **electromagnetic spin-orbit** correction to the nucleon single-particle energy (non-relativistic),

$$\varepsilon_i^{emso} = \frac{\hbar^2c^2}{2m_i^2c^4}\langle\vec{l}_i\cdot\vec{s}_i\rangle x_i \int \frac{1}{r}\frac{dU_C}{dr}|R_i(r)|^2$$

where x_i: $g_p - 1$ for Z and g_n for N; $g_n = -3.82608545(90)$ and $g_p = 5.585694702(17)$, $R_i \to R_{nl}$ radial wf.

• **Finite size** effects (assuming spherical symmetry):

$$\begin{aligned}\rho_{ch}(q) &= \left(1-\frac{q^2}{8m^2}\right)\left[G_{E,p}(q^2)\rho_p(q)+G_{E,n}(q^2)\rho_n(q)\right] \\ &- \frac{\pi q^2}{2m^2}\sum_{l,t}\left[2G_{M,t}(q^2)-G_{E,t}(q^2)\right]\langle\vec{l}\cdot\vec{s}\rangle\int_0^\infty dx\frac{j_1(qx)}{qx}|R_{nl}(x)x^2|^2\end{aligned}$$

• The lowest order correction in the fine-structure constant to the Coulomb potential $\frac{eZ}{r}$ consists on the selfenergy and the **vacuum polarization** corrections:

$$V_{vp}(\vec{r}) = -\frac{2}{3}\frac{\alpha e^2}{\pi}\int d\vec{r}'\frac{\rho(\vec{r}')}{|\vec{r}-\vec{r}'|}\mathcal{K}_1\left(\frac{2}{\lambda\!\!\!^{-}_e}|\vec{r}-\vec{r}'|\right)$$

where e is the fundamental electric charge, α the fine-structure constrant, $\lambda\!\!\!^{-}_e$ the reduced Compton electron wavelength and

$$\mathcal{K}_1(x) \equiv \int_1^\infty dt e^{-xt}\left(\frac{1}{t^2}+\frac{1}{2t^4}\right)\sqrt{t^2-1}$$

Isospin proposed by J. Heisenberg

Isospin conservation $[H,T]=0$

$$[H,T]=[V_C+V_{CSB}+V_{CIB},T]\neq 0$$

Scattering Length

$$a^{pp}_{(S=0)} = -17.3\pm 0.4\mathrm{fm},$$
$$a^{nn}_{(S=0)} = -18.7\pm 0.6\mathrm{fm},$$
$$a^{pn}_{(S=0)} = -23.70\pm 0.03\mathrm{fm}.$$

The difference between a_0^{pp} and a_0^{nn} is an evidence of CSB (charge symmetry breaking) nuclear force, while the difference between a_0^{pn} and the average $(a_0^{pp}+a_0^{nn})/2$ is due to CIB (charge invariance breaking) force.

CSB and CIB in Lattice QCD calculations in future project

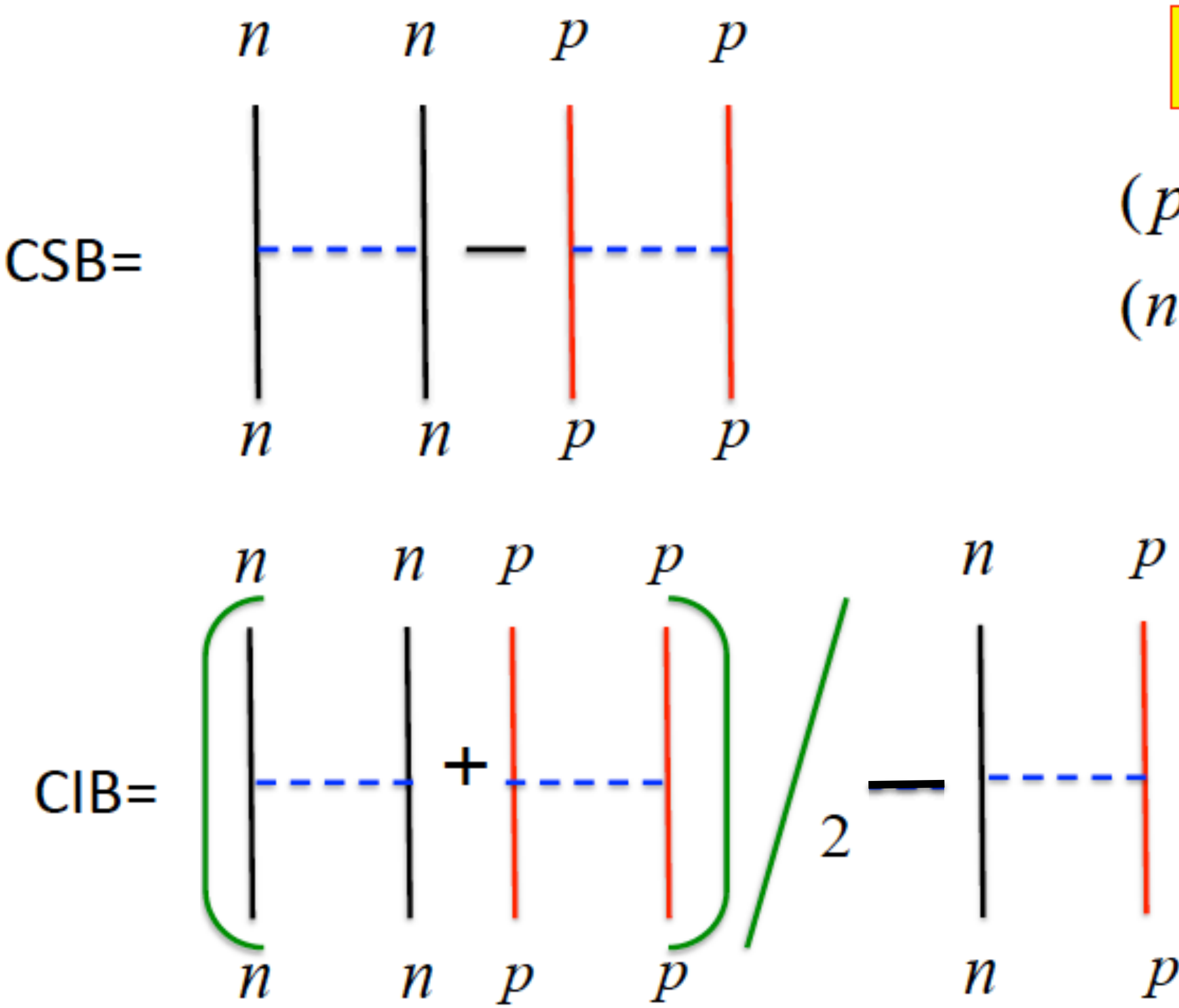

QCD

$$(p) = (uud)$$

$$(n) = (udd)$$

$$m_u \neq m_d$$

$$q_u \neq q_d$$

$$\Delta a_{CSB} = 1.4$$

$$\Delta a_{CIB} = 5.7$$

- **Isospin symmetry breaking** (Skyrme-like): **two parts**

H. Sagawa, N. V. Giai, and T. Suzuki, Phys. Lett. B **353**, 7 (1995).

charge symmetry breaking + **charge independence breaking***

$$V_{CSB} = V_{nn} - V_{pp}$$

$$V_{CIB} = \frac{1}{2}(V_{nn} + V_{pp}) - V_{pn}$$

$$V_{CSB}(\vec{r}_1, \vec{r}_2) \equiv \frac{1}{4}[\tau_z(1) + \tau_z(2)]\Big\{ s_0(1 + y_0 P_\sigma)\,\delta(\vec{r}_1 - \vec{r}_2) + \frac{1}{2}s_1(1 + y_1 P_\sigma)\left[P'^2\delta(\vec{r}_1 - \vec{r}_2) + \delta(\vec{r}_1 - \vec{r}_2)P^2\right] + s_2(1 + y_2 P_\sigma)\vec{P}'\cdot\delta(\vec{r}_1 - \vec{r}_2)\vec{P}\Big\}$$

where $\vec{P} \equiv \frac{1}{2\imath}(\vec{\nabla}_1 - \vec{\nabla}_2)$ acts on the right and P' is its complex conjugate acting on the left and $P_{\tau/\sigma}$ are the usual projector operators in isospin and spin spaces.

$$V_{CIB}(\vec{r}_1, \vec{r}_2) \equiv \frac{1}{2}\tau_z(1)\tau_z(2)\Big\{ u_0(1 + z_0 P_\sigma)\,\delta(\vec{r}_1 - \vec{r}_2) + \frac{1}{2}u_1(1 + z_1 P_\sigma)\left[P'^2\delta(\vec{r}_1 - \vec{r}_2) + \delta(\vec{r}_1 - \vec{r}_2)P^2\right] + u_2(1 + z_2 P_\sigma)\vec{P}'\cdot\delta(\vec{r}_1 - \vec{r}_2)\vec{P}\Big\}$$

* general operator form $\tau_z(1)\tau_z(2) - \frac{1}{3}\vec{\tau}(1)\cdot\vec{\tau}(2)$. Our prescription $\tau_z(1)\tau_z(2)$ not change structure of HF+RPA.

- Opposite to the other corrections, **ISB contributions depends on new parameters that need to be fitted!**

Isospin symmetry breaking in the medium:

- keeping things simple: CSB and CIB interaction just delta function depending on s_0 and u_0. Different possibilities:

→ Fitting to (two) experimentally known IAS energies

→ Derive from theory

→ our option: u_0 to reproduce BHF (symmetric nuclear matter) and s_0 to reproduce E_{IAS} in ^{208}Pb

$$\Delta E_{ISB} \propto u_0 \rho^2$$

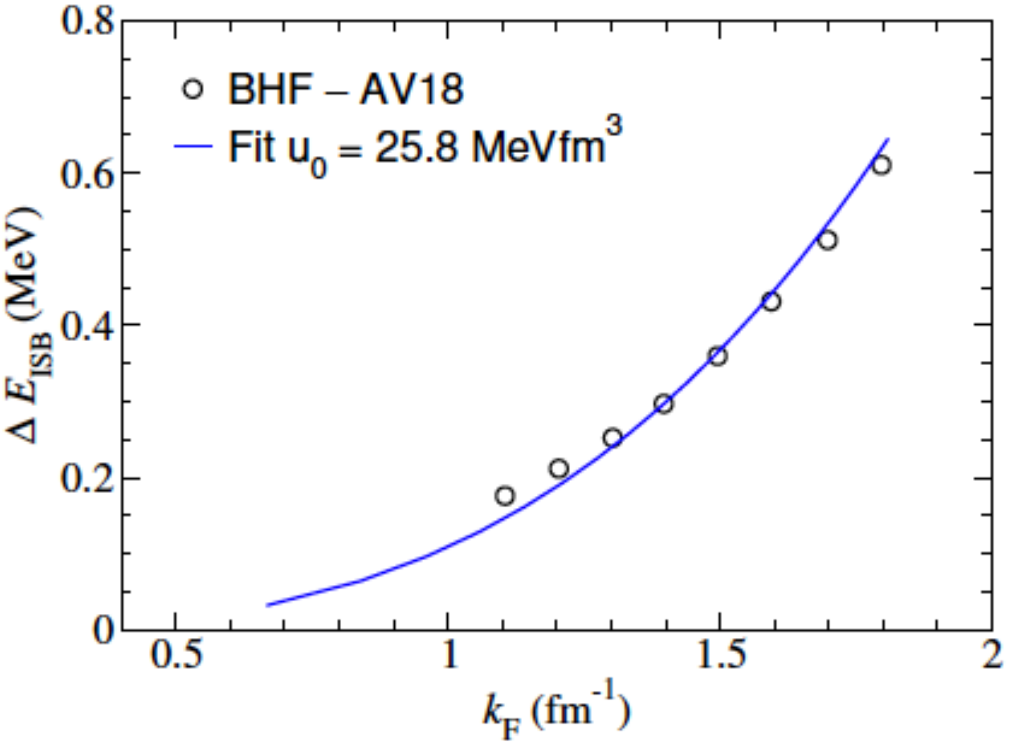

Physics Letters B 445, 259 (1999)

Example: 2 different fitting protocols and models:

SLy5-min: use constant error for a given observable

- **Binding energies** of ^{40,48}Ca, ^{56}Ni, ^{130,132}Sn and ^{208}Pb with a fixed adopted error of **2 MeV**
- the **charge radius** of ^{40,48}Ca, ^{56}Ni and ^{208}Pb with a fixed adopted error of **0.02 fm**
- the **neutron matter** Equation of State calculated by Wiringa *et al.* (1988) for densities between 0.07 and 0.40 fm^{-3} with an adopted error of **10%**
- the **saturation energy** ($e(\rho_0) = -16.0 \pm 0.2$ MeV) and **density** ($\rho_0 = 0.160 \pm 0.005$ fm^{-3}) of symmetric nuclear matter.

DD-ME-min1: use relative error for all observables

- **binding energies, charge radii, diffraction radii and surface thicknesses** of 17 even-even spherical nuclei, ^{16}O, ^{40,48}Ca, ^{56,58}Ni, ^{88}Sr, ^{90}Zr, ^{100,112,120,124,132}Sn, ^{136}Xe, ^{144}Sm and ^{202,208,214}Pb. The assumed errors of these observables are **0.2%, 0.5%, 0.5%, and 1.5%**, respectively.

Re-fit of SAMi: SAMi-ISB

- All these **corrections** are relatively **small** but **modify binding energies, neutron and proton distributions, etc.**

$\Rightarrow$ a **re-fit of the interaction is needed**.

- Use **SAMi fitting protocol** (special care for spin-isospin resonances) including all corrections and **find SAMi-ISB**

Table: Saturation properties

	SAMi	SAMi-ISB	
ρ_∞	0.159(1)	0.1613(6)	fm^{-3}
e_∞	−15.93(9)	−16.03(2)	MeV
m^*_{IS}	0.6752(3)	0.730(19)	
m^*_{IV}	0.664(13)	0.667(120)	
J	28(1)	30.8(4)	MeV
L	44(7)	50(4)	MeV
K_∞	245(1)	235(4)	MeV

TABLE I. SAMi-ISB parameter set used in the fit. See text for details.

e_0	-16.03(2) MeV	L	50(5) MeV
ρ_0	0.1613(6) MeV	$m^*_{\rm IS}/m$	0.730(19)
K_0	235(4) MeV	$m^*_{\rm IV}/m$	0.667(116)
J	30.8(4) MeV	G_0	0.15(fixed)
W_0	294(6)	G'_0	0.35(fixed)
W'_0	−367(12)		
s_0	−26.3(7) MeV fm^3	u_0	25.8(4) MeV fm^3

TABLE II. SAMi-ISB in terms of Skyrme standard parameters. See text for details.

	value(σ)		value(σ)
t_0	−2098.3(149.3) MeV fm^3	x_0	0.24(9)
t_1	394.7(15.8) MeV fm^5	x_1	−0.17(33)
t_2	−136.4(10.8) MeV fm^5	x_2	−0.47(4)
t_3	11995(686) MeV fm$^{3+3\alpha}$	x_3	0.32(21)
W_0	294(6)		
W'_0	−367(12)	s_0	−26.3(7) MeV fm^3
α	0.223(31)	u_0	25.8(4) MeV fm^3

SAMi-ISB finite nuclei properties

El.	N	B [MeV]	B^{exp} [MeV]	r_c [fm]	r_c^{exp} [fm]	ΔR_{np} [fm]
Ca	28	417.67	415.99	3.49	3.47	0.214
Zr	50	783.60	783.89	4.26	4.27	0.097
Sn	82	1102.75	1102.85	4.73	–	0.217
Pb	126	1635.78	1636.43	5.50	5.50	0.151

Corrections on E_{IAS} for ^{208}Pb one by one

	E_{IAS} [MeV]	Correction [keV]
No corrections[a]	18.31	
Exact Coulomb exchange	18.41	+100
n/p mass difference	18.44	+30
Electromagnetic spin-orbit	18.45	+10
Finite size effects	18.40	-50
Vacuum polarization (V_{ch})	18.53	+130
Isospin symmetry breaking	18.80	+270

[a] From Skyrme Hamiltonian where the nuclear part is isospin symmetric and V_{ch} is calculated from the ρ_p

$E_{IAS}^{exp} = 18.826 \pm 0.01$ MeV. *Nuclear Data Sheets 108, 1583 (2007).*

E_{IAS} with SAMi-ISB

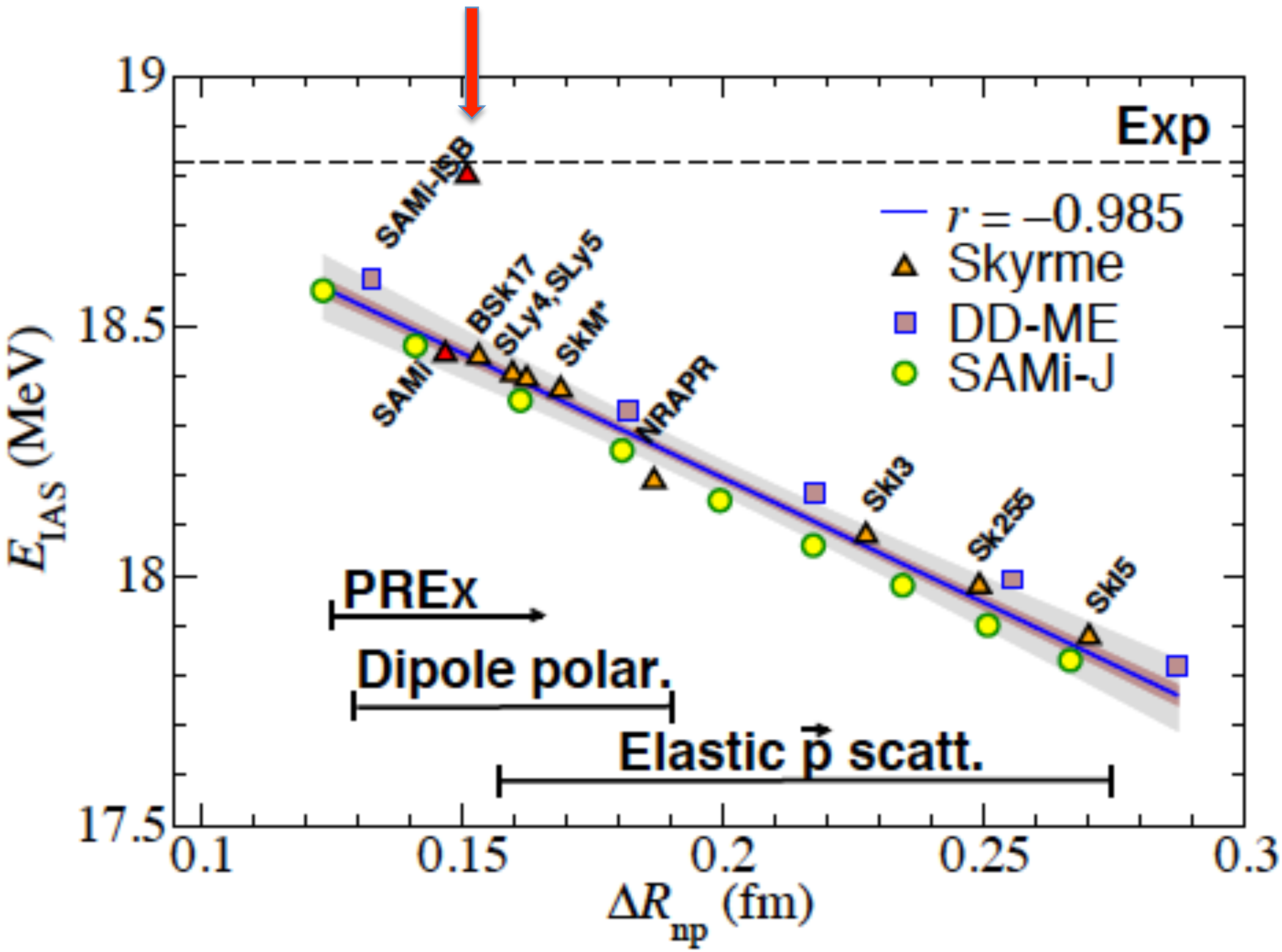

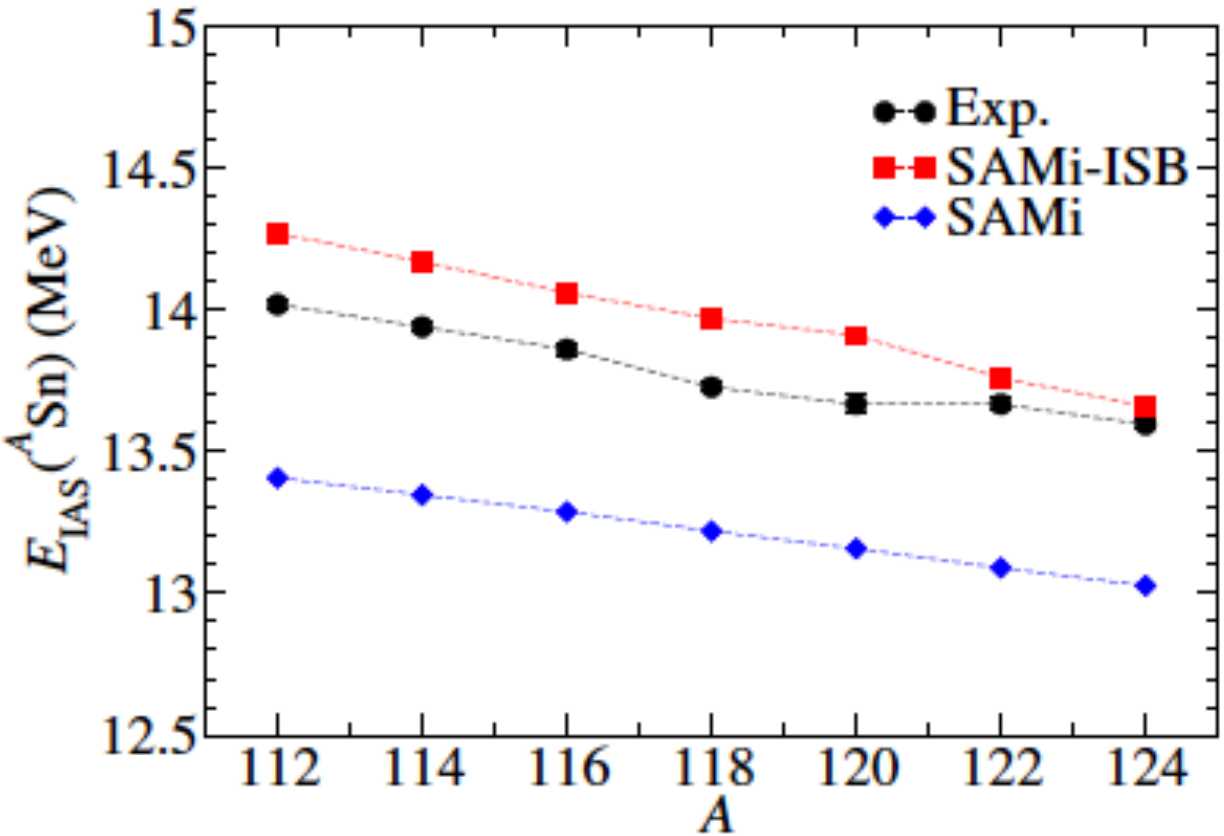

FIG. 3. $E_{\rm IAS}$ for Sn isotopes as predicted by SAMi and SAMi-ISB and compared to experimental data.

Isospin-symmetry breaking in masses of $N \simeq Z$ nuclei

P. Bączyk[a,*], J. Dobaczewski[a,b,c,d], M. Konieczka[a], W. Satuła[a,d], T. Nakatsukasa[e], K. Sato[f]

Physics Letters B 778 (2018) 178–183

Mirror Displacement energy

$$\mathrm{MDE} = BE(T, T_z = -T) - BE(T, T_z = +T). \qquad (1)$$

Triplet displacement energy

$$\mathrm{TDE} = BE(T = 1, T_z = -1) + BE(T = 1, T_z = +1) - 2BE(T = 1, T_z = 0), \qquad (2)$$

$$\hat{V}^{\mathrm{II}}(i, j) = t_0^{\mathrm{II}} \delta(\mathbf{r}_i - \mathbf{r}_j)\left[3\hat{\tau}_3(i)\hat{\tau}_3(j) - \hat{\vec{\tau}}(i) \circ \hat{\vec{\tau}}(j)\right] \quad \text{(CIB)}$$

$$\hat{V}^{\mathrm{III}}(i, j) = t_0^{\mathrm{III}} \delta(\mathbf{r}_i - \mathbf{r}_j)\left[\hat{\tau}_3(i) + \hat{\tau}_3(j)\right]. \quad \text{(CSB)}$$

Isospin projected HF calculations

Isospin-symmetry breaking in masses of $N \simeq Z$ nuclei

P. Bączyk [a,*], J. Dobaczewski [a,b,c,d], M. Konieczka [a], W. Satuła [a,d], T. Nakatsukasa [e], K. Sato [f]

Physics Letters B 778 (2018) 178–183

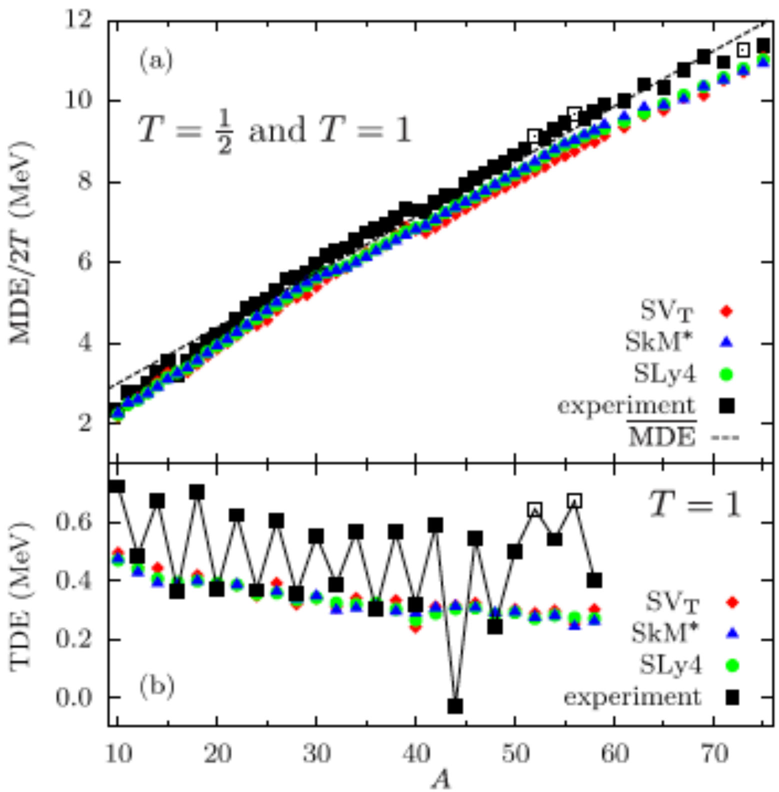

Fig. 1. (Color online.) Calculated (no ISB terms) and experimental values of MDEs (a) and TDEs (b). The values of MDEs for triplets are divided by two to fit in the plot. Thin dashed line shows the average linear trend of experimental MDEs in doublets, defined as $\overline{MDE} = 0.137A + 1.63$ (in MeV). Measured values of binding energies were taken from Ref. [25] and the excitation energies of the $T = 1$, $T_z = 0$ states from Ref. [26]. Open squares denote data that depend on masses derived from systematics [25].

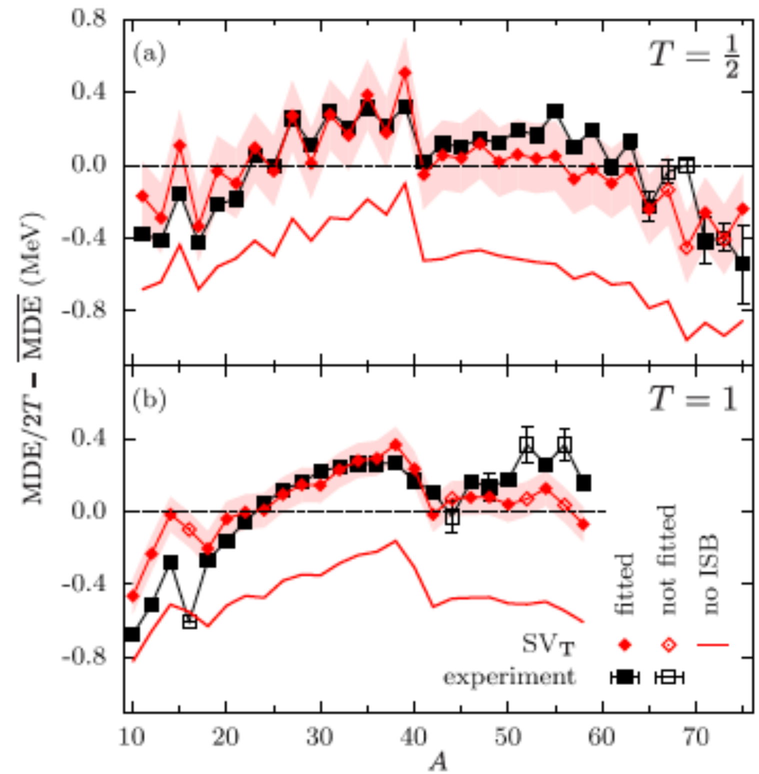

Fig. 2. (Color online.) Calculated and experimental [25] values of MDEs for the $T = \frac{1}{2}$ (a) and $T = 1$ (b) mirror nuclei, shown with respect to the average linear trend defined in Fig. 1. Calculations were performed for functional SV_T^{ISB}. Shaded bands show theoretical uncertainties, evaluated according to the methodology discussed in detail in the Supplemental Material [22]. Experimental error bars are shown only when they are larger than the corresponding symbols. Full (open) symbols denote data points included in (excluded from) the fitting procedure.

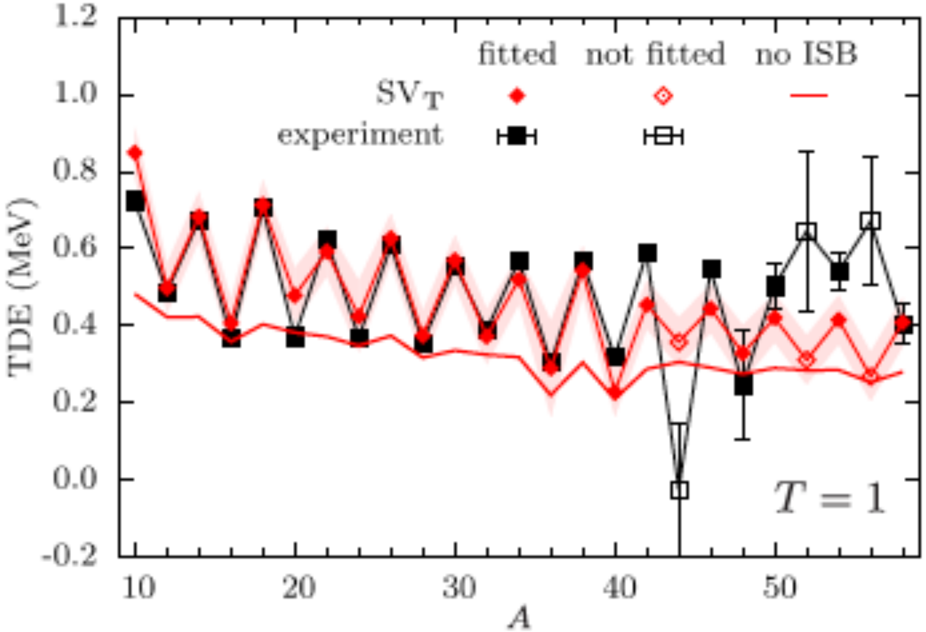

Fig. 3. (Color online.) Same as in Fig. 2 but for the $T = 1$ TDEs with no linear trend subtracted.

Isospin-symmetry breaking in masses of $N \simeq Z$ nuclei

P. Bączyk[a,*], J. Dobaczewski[a,b,c,d], M. Konieczka[a], W. Satuła[a,d], T. Nakatsukasa[e], K. Sato[f]

Physics Letters B 778 (2018) 178–183

$$\mathrm{MDE} = BE(T, T_z = -T) - BE(T, T_z = +T). \quad (1)$$

$$\mathrm{TDE} = BE(T = 1, T_z = -1) + BE(T = 1, T_z = +1) - 2BE(T = 1, T_z = 0), \quad (2)$$

$$\hat{V}^{\mathrm{II}}(i,j) = t_0^{\mathrm{II}} \delta\left(\boldsymbol{r}_i - \boldsymbol{r}_j\right)\left[3\hat{\tau}_3(i)\hat{\tau}_3(j) - \hat{\vec{\tau}}(i) \circ \hat{\vec{\tau}}(j)\right] \quad \text{(CIB)}$$

$$\hat{V}^{\mathrm{III}}(i,j) = t_0^{\mathrm{III}} \delta\left(\boldsymbol{r}_i - \boldsymbol{r}_j\right)\left[\hat{\tau}_3(i) + \hat{\tau}_3(j)\right]. \quad \text{(CSB)}$$

Coupling constants t_0^{II} and t_0^{III} and their uncertainties obtained in this work for the Skyrme EDFs $\mathrm{SV}_{\mathrm{T}}^{\mathrm{ISB}}$, $\mathrm{SkM}^{*\mathrm{ISB}}$, and $\mathrm{SLy4}^{\mathrm{ISB}}$. In the last row we show their corresponding ratios.

	$\mathrm{SV}_{\mathrm{T}}^{\mathrm{ISB}}$	$\mathrm{SkM}^{*\mathrm{ISB}}$	$\mathrm{SLy4}^{\mathrm{ISB}}$	Ours	
t_0^{II} (MeV fm^3)	4.6 ± 1.6	7 ± 4	6 ± 4	$u_0/2$	12.9
t_0^{III} (MeV fm^3)	-7.4 ± 1.9	-5.6 ± 1.4	-5.6 ± 1.1	$S_0/2$	-13.1
$t_0^{\mathrm{II}}/t_0^{\mathrm{III}}$	-0.6 ± 0.3	-1.3 ± 0.8	-1.1 ± 0.7		-0.985

CSB and CIB from $^1S_0$ NN scattering => scattering length
(T. Suzuki et at., PRC47, R1360 (1993))

$$s_0 \propto -\Delta a_{CSB}$$

$$u_0 \propto \frac{2}{3}\Delta a_{CIB}$$

$$\frac{u_0}{s_0} = -2.5$$

The ratio of adjusted CSB and CIB is 2-3 times smaller than the above value. The adjusted values may include the effect of Coulomb correlations beyond mean field and also many-body ISB correlations.

Summary

1. Skyrme and RMF EDF show a strong correlation between E_{IAS} and neutron skin of ^{208}Pb. However, EDF does not properly describe the excitation energy of IAS.
2. Refitted EDF with CSB and CIS gives good account of both E_{IAS} and other ground state observables, BE, charge radii, neutron skin.
3. Mass measurements of isospin doublet and triplets give complementary information of CSB and CIB interactions.
4. A better knowledge of CSB and CIS in nuclear medium gives a further enhancement of nuclear matter properties, EoS and symmetry energy.

Isobaric analog state of ^{11}Li

T. Teranishi [a,1], S. Shimoura [b], Y. Ando [b], M. Hirai [c], N. Iwasa [b,2], T. Kikuchi [b], S. Moriya [b], T. Motobayashi [b], H. Murakami [b], T. Nakamura [c], T. Nishio [b], H. Sakurai [a], T. Uchibori [b], Y. Watanabe [a], Y. Yanagisawa [b], M. Ishihara [a,c]

[a] The Institute of Physical and Chemical Research (RIKEN), 2-1 Hirosawa, Wako, Saitama 351-01, Japan
[b] Department of Physics, Rikkyo University, 3 Nishi-Ikebukuro, Toshima, Tokyo 171, Japan
[c] Department of Physics, University of Tokyo, 7-3-1 Hongo, Bunkyo, Tokyo 113, Japan
[d] GSI, Planckstrasse 1, D-64291 Darmstadt, Germany

Received 19 March 1997; revised manuscript received 2 June 1997
Editor: R.H. Siemssen

^{11}Li(p,n)^{11}Be*

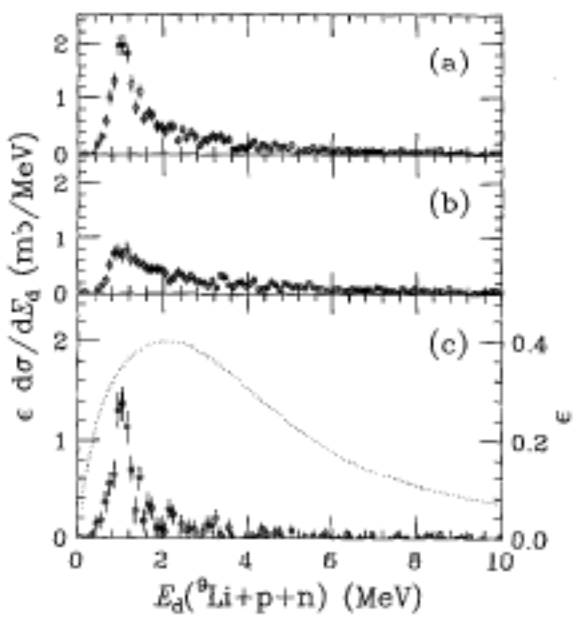

Fig. 2. Decay energy (E_d) spectra of the ^{9}Li+p+n system (a) for the (p,n) reaction and (b) for the (d,2n) reaction. (c) Decay energy spectrum of the ^{9}Li+p+n system deduced for the Fermi transition (see text). The dotted line represents the detector acceptance ε.

PHYSICAL REVIEW C **86**, 041307(R) (2012)

Double isobaric analog of ^{11}Li in ^{11}B

R. J. Charity,[1] L. G. Sobotka,[1] K. Hagino,[2] D. Bazin,[3] M. A. Famiano,[4] A. Gade,[3] S. Hudan,[5] S. A. Komarov,[1] Jenny Lee,[3] S. P. Lobastov,[3] S. M. Lukyanov,[3] W. G. Lynch,[3] C. Metelko,[5] M. Mocko,[3] A. M. Rogers,[3] H. Sagawa,[6,7] A. Sanetullaev,[3] M. B. Tsang,[3] M. S. Wallace,[3] M. J. van Goethem,[8] and A. H. Wuosmaa[4]

^{12}Be$(p,2n)^{11}$B ı

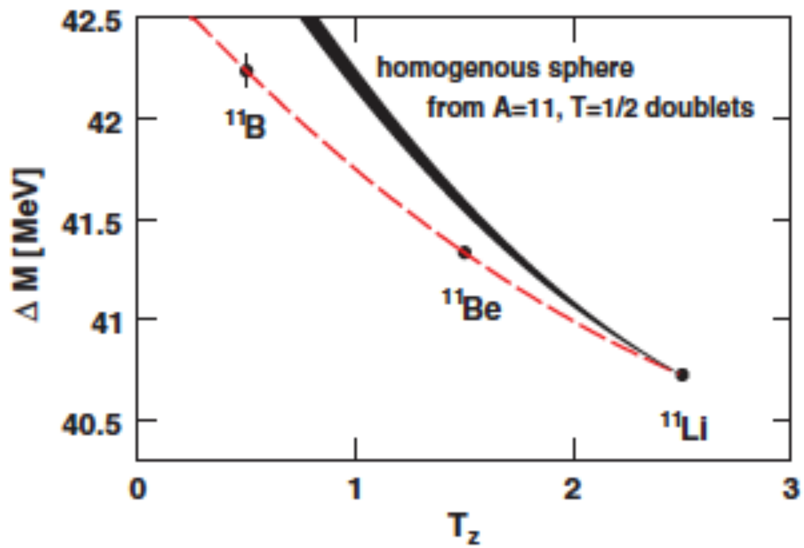

FIG. 2. (Color online) Mass excesses of the three known members of the $A = 11$ sextet plotted as a function of isospin projection. The solid band shows the prediction for a homogeneous sphere with the same radius as the $T = 1/2$, $A = 11$ doublet. The dashed curve shows the quadratic IMME curve which passes through the three data points.

a secondary ^{12}Be beam at $E/A = 50$ MeV produced at the coupled-cyclotron facility at the National Superconducting Cyclotron Laboratory at Michigan State University. See

TABLE IV. E_{IAS} and r_{ch} for some selected nuclei as predicted by SAMi and SAMi-ISB, as well as the experimental values and errors (within parenthesis).

		SAMi		SAMi-ISB		Experiment	
El.	N	E_{IAS} [MeV]	r_{ch} [fm]	E_{IAS} [MeV]	r_{ch} [fm]	E_{IAS} [MeV]	r_{ch} [fm]
Ca	28	6.573	3.525	6.79(2)	3.497(3)	7.182(8)	3.477(2)
Zr	50	11.199	4.283	11.36(4)	4.262(3)	11.901(12)	4.269(1)
Sn	112	13.408	4.539	14.27(3)	4.611(3)	14.019(20)	4.595(2)
	114	13.347	4.553	14.17(3)	4.619(3)	13.940(20)	4.610(2)
	116	13.288	4.567	14.06(3)	4.633(3)	13.861(20)	4.625(2)
	118	13.220	4.582	13.97(3)	4.647(3)	13.728(17)	4.639(2)
	120	13.158	4.596	13.91(3)	4.659(2)	13.667(32)	4.652(2)
	122	13.090	4.610	13.76(3)	4.671(2)	13.667(20)	4.663(2)
	124	13.027	4.623	13.66(3)	4.684(2)	13.596(20)	4.673(2)
Pb	126	18.256	5.517	18.80(5)	5.507(2)	18.826(10)	5.501(1)